inorganics

MDPI

Article

Cd(II)-Based Coordination Polymers and Supramolecular Complexes Containing Dianiline Chromophores: Synthesis, Crystal Structures, and Photoluminescence Properties

Nicoleta Craciun [1], Elena Melnic [1], Anatolii V. Siminel [1], Natalia V. Costriucova [1], Diana Chisca [2] and Marina S. Fonari [1,*]

[1] Institute of Applied Physics, Moldova State University, Academiei 5, MD-2028 Chișinău, Moldova; nicoletacaimac@gmail.com (N.C.); elena.melnic2@gmail.com (E.M.); ansiminel@gmail.com (A.V.S.); ncostriucova@gmail.com (N.V.C.)

[2] Faculty of Biology and Chemistry, Ion Creangă State Pedagogical University of Chișinău, Ion Creangă 1, MD-2069 Chișinău, Moldova; chisca.diana@upsc.md

* Correspondence: fonari.xray@gmail.com

Abstract: Five new coordination compounds that included three coordination polymers and two supramolecular complexes were obtained by reactions of different cadmium salts (tetrafluoroborate, nitrate, and perchlorate) with dianiline chromophores, 4,4′-diaminodiphenylmethane (ddpm), and 4,4′-diaminodiphenylethane (ddpe). The crystal structures were studied by single-crystal X-ray analysis. The coordination arrays with the ddpm chromophore included $\{[Cd(OH)(H_2O)(ddpm)_2](BF_4)\}_n$ (**1**) as a one-dimensional (1D) coordination garland chain, $\{[Cd(NO_3)(ddpm)_2](H_2O)(NO_3)\}_n$ (**2**) as a two-dimensional (2D) coordination layer, and $[Cd(bpy)_2(ddpm)_2](ddpm)(NO_3)_2$ (**3**) as a supramolecular complex. The products with the ddpe chromophore were identified as $\{[Cd(phen)_2(ddpe)](ClO_4)_2\}_n$ (**4**) in the form of a linear coordination chain and $[Cd(phen)_3](ClO_4)_2(ddpe)_{0.5}(CH_3CN)_{0.5}$ (**5**) as a supramolecular complex. The extension of coordination arrays in **1**, **2**, and **4** was achieved via dianiline ligands as bidentate linkers and additionally via bridging of nitrate anions in **2**. The diversification of products became possible due to usage of 2,2′-bipyridine (bpy) and 1,10-phenanthroline (phen) as co-ligands forming the terminal corner fragments $[Cd(bpy)_2]^{2+}$, $[Cd(phen)_2]^{2+}$, and $[Cd(phen)_3]^{2+}$ in **3**–**5**, respectively. The assembling of coordination entities occurred via the interplay of hydrogen bonds with the participation of amino groups, water molecules, and inorganic anions. Two dianilines were powerful luminophores in the crystalline phase, while the photoluminescence in **1**–**5** was considerably weaker than in the pure ddpm and ddpe luminophores and redistributed along the spectrum.

Keywords: 4,4′-diaminodiphenylmethane; 4,4′-diaminodiphenylethane; cadmium; IR spectroscopy; X-ray; photoluminescence

check for updates

Academic Editor: Iolinda Aiello

Received: 19 February 2025
Revised: 8 March 2025
Accepted: 12 March 2025
Published: 18 March 2025

Citation: Craciun, N.; Melnic, E.; Siminel, A.V.; Costriucova, N.V.; Chisca, D.; Fonari, M.S. Cd(II)-Based Coordination Polymers and Supramolecular Complexes Containing Dianiline Chromophores: Synthesis, Crystal Structures, and Photoluminescence Properties. *Inorganics* **2025**, *13*, 90. https://doi.org/10.3390/inorganics13030090

Copyright: © 2025 by the authors. Licensee MDPI, Basel, Switzerland. This article is an open access article distributed under the terms and conditions of the Creative Commons Attribution (CC BY) license (https://creativecommons.org/licenses/by/4.0/).

1. Introduction

The analysis the of landscapes of different types of interactions is important for crystal engineering and understanding the stability of new multifunctional materials. The advantages of synergism of coordination and hydrogen bonds within the same supramolecular network displaying improved mechanical strength, stability, and elasticity of the supramolecular array were reported [1–6]. The combination of coordination and hydrogen bonds allowed for controlling and tuning the rigidity/flexibility of supramolecular networks. It is a reliable way to either diversify the coordination aggregates or to obtain

the reproducible structural motifs, with the possibility to induce and tune the properties intentionally. In particular, the materials based on coordination bonds and strong hydrogen bonds exhibited zeolite-like properties, imitating the rigid coordination frameworks while being dynamic adsorbents of guest molecules. The were larger than diatomic gases, which was crucial for environmental and separation issues, providing the retention/separation of volatile organic compounds (VOCs), solvents, and toxic molecules [7–11]. In this regard, the molecules bearing the terminal amino groups are of a great importance. In our group, we focused on the synergism of coordination and hydrogen bonds in coordination polymers, where the combination of transition metals with organic H-donor molecules resulted in crystalline solids with potential optical and adsorption applications [11]. The synergism of coordination and hydrogen bonds was also successfully used for the preparation of new supramolecular elastomer materials with self-recovery capability and self-healing properties, revealing their potential applications in the biomedical field [12–14]. In the reported systems, the hydrogen bonds achieved rapid reformation after fracture and dissipated the strain energy as weak dynamic bonds, giving the elastomer self-healing and high stretch abilities, while the coordination bonds contributed to the robust molecular networks and led to significantly improved robustness and elasticity. It was documented that the most intriguing results were obtained in the systems that combined different types of dynamic bonds [12–14].

Along with other studies [15–18], our recent interest in aniline chromophores was stimulated by their ditopic functions, since the amino groups are capable of acting both as coordination sites and H-bonded sites, thus serving as suitable building blocks for the construction of coordination entities, coordination polymers in particular, as they are additionally stabilized by H-bonded networks [19–21]. Furthermore, aniline derivatives also possess good photoelectric and processing properties, designability, and pH sensitivity [22–26]. It was reported that the functionalization of the linear aniline derivatives aimed at the restriction of intramolecular motion (RIM) was an effective method for their ACQ-AIE (aggregation-caused quenching–aggregation-induced emission) conversion [22]. Otherwise, numerous anilines and their derivatives were reported as chemical modifiers and regulators to control the emission of quantum dots (QDs) [24–26].

In continuation of our recent research, the present study is focused on the coordination chemistry of two semirigid dianiline chromophores, 4,4′-diaminodiphenylmethane (ddpm) and 4,4′-diaminodiphenylethane (ddpe), with a range of cadmium(II) salts (tetrafluoroborate, nitrate, perchlorate). We aim at better understanding how the resulting coordination networks can be manipulated by both the degrees of conformational freedom in the ligand and by utilizing different anions. To diversify the structural landscape of coordination compounds with the participation of two dianiline chromophores, a number of reactions were carried out in the presence of the co-reactants, 2,4-diamino-6-phenyl-1,3,5-triazine as a competing amino ligand, or 2,2′-bipyridine and 1,10-phenanthroline as strong chelating agents and weak luminophores [27–29]. The synthetic protocols, single-crystal X-ray structures, and spectroscopic properties were reported for five new coordination compounds, {[Cd(OH)(H_2O)(ddpm)$_2$](BF_4)}$_n$ (**1**), {[Cd(NO_3)(ddpm)$_2$](H_2O)(NO_3)}n (**2**), [Cd(bpy)$_2$(ddpm)$_2$](ddpm)(NO_3)$_2$ (**3**), {[Cd(phen)$_2$(ddpe)](ClO_4)$_2$}$_n$ (**4**), and [Cd(phen)$_3$](ClO_4)$_2$(ddpe)$_{0.5}$(CH_3CN)$_{0.5}$ (**5**).

2. Results and Discussion

2.1. General Process

The reported compounds **1**–**5** were prepared by reactions of cadmium salts with two dianiline chromophores, 4,4′-diaminodiphenylmethane (ddpm) and 4,4′-diaminodiphenylethane (ddpm), in the presence of co-reactants (2,4-diamino-6-phenyl-1,3,5-triazine, 2,2′-bipyridine

(bpy), and 1,10-phenanthroline (phen)) (see Section 3) and under soft synthetic conditions. In the case of the triazine/ddpm pair, ddpm exclusively coordinated to the metal in **1** and **2**, while in the case of the bpy/phen co-reactants, the simultaneous coordination of N-bases with different strengths was reached in **3** and **4**. The reactions were carried out in a mixture of MeCN: EtOH or in EtOH as a solvent.

2.2. IR Characterization

The IR spectra for the ligands and compounds **1**–**5** are depicted in Figure 1, Figure 2 and Figures S1–S5 and are also listed in Table S1. In the ligands, the characteristic bands at 3443 and 3335 cm^{-1} were assigned to the stretching vibration of the primary amino groups. Compounds **1**–**5** revealed the asymmetric and symmetric stretching vibrations ν_{as}(NH) and ν_{s}(NH) in the 3340–3156 cm^{-1} regions, which agrees with the reported data for the coordinated and uncoordinated NH_2 groups [30]. A strong signal for the C–H in-plane bending vibration was registered at 1627–1575 cm^{-1} in the ligands and in the 1664–1560 cm^{-1} region for **1**–**5**. The deformation vibrations of the aliphatic and aromatic C–H groups were present at 956–491 cm^{-1}. The BF_4^- anion in **1** was registered as strong signals in the range of 1054–1019 cm^{-1}, with the splitting depending on the local asymmetry due to interacting species [31]. The N–O stretching appeared as strong splitting bands in the range of 1079–1015 cm^{-1} and a weak band at 1280 cm^{-1} in **2**, while it appeared as a strong band at 1306 cm^{-1} and a weak one at 1024 cm^{-1} in **3** [32]. The perchlorate anions appeared as a very strong band, assigned to the antisymmetric stretching mode of the Cl–O bond, which was split as 1090, 1054, and 1019 cm^{-1} in **4**, and centered at 1077 cm^{-1} in **5** [33]. This asymmetric band shape was the sequence of the geometry distortion.

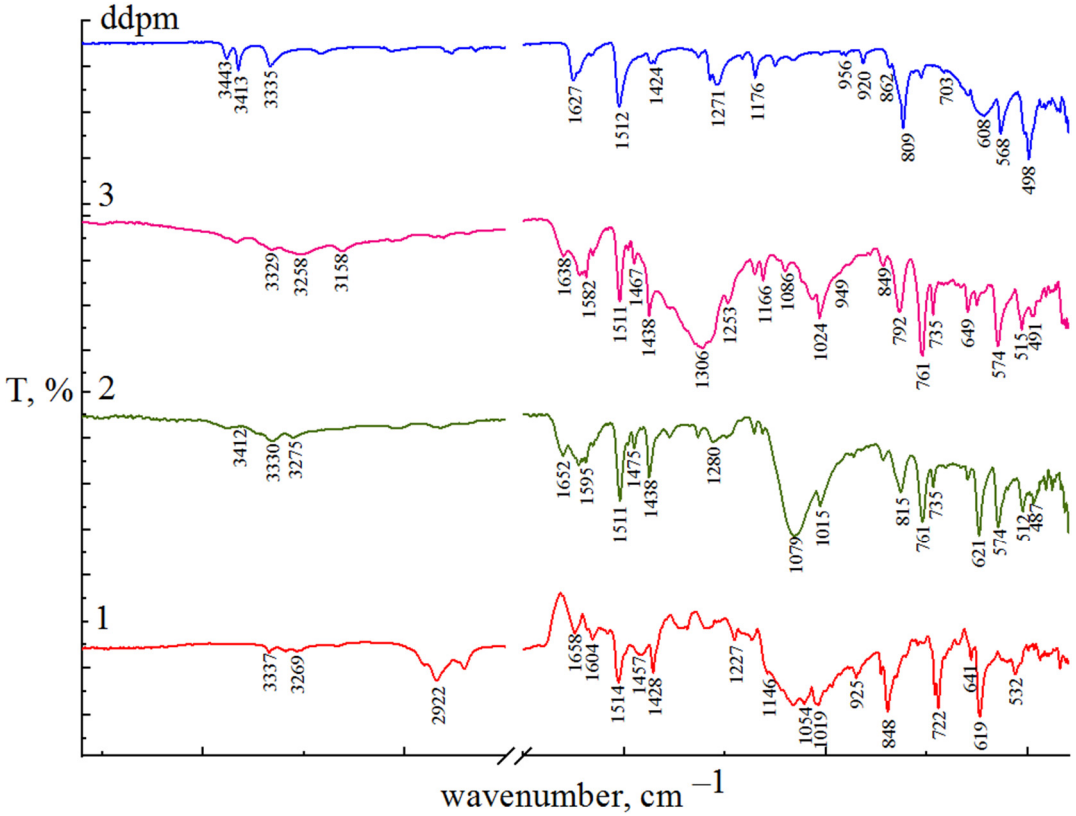


Figure 1. IR spectra of compounds **1**, **2**, and **3** and ddpm ligand.

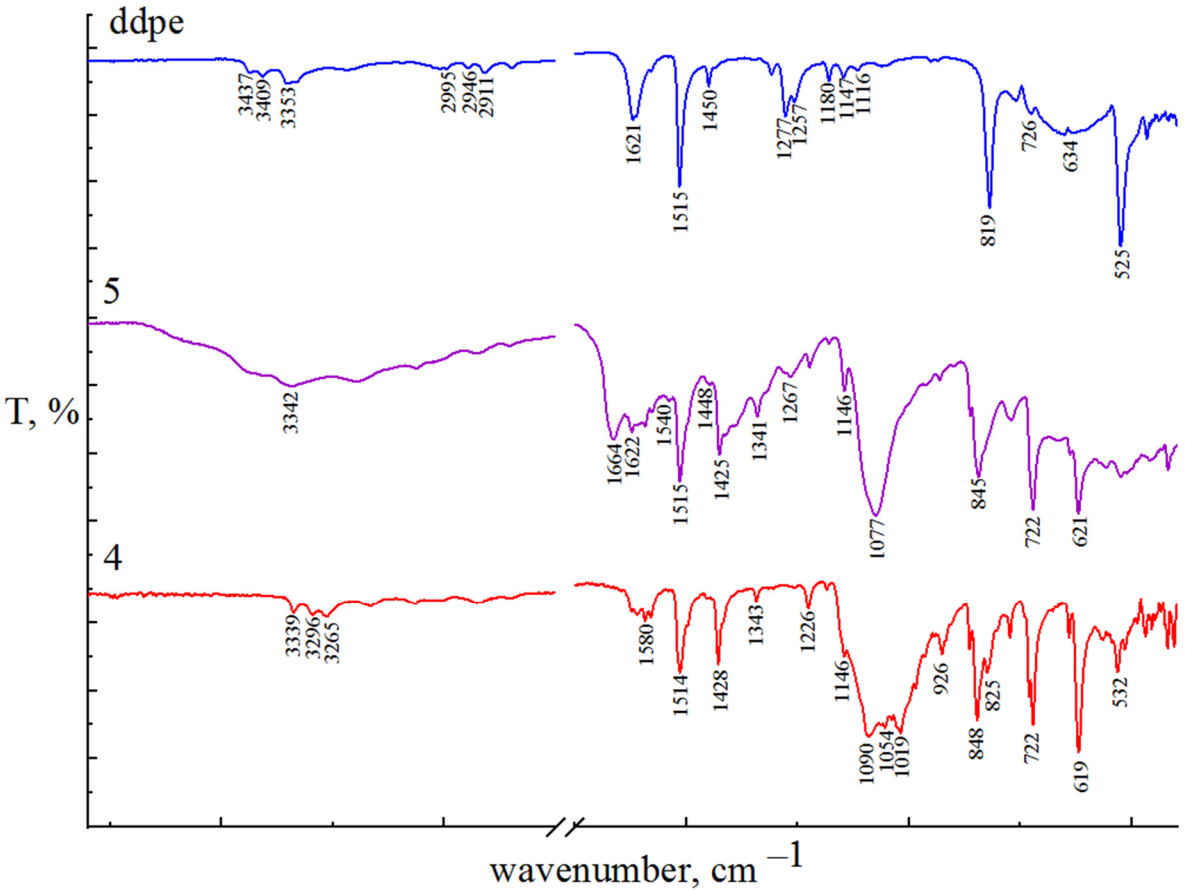


Figure 2. IR spectra of compounds **4** and **5** and ddpe ligand.

2.3. X-Ray Study

The structures of **1**–**5** were unambiguously confirmed by single-crystal X-ray analysis. The crystal purity in bulk was confirmed by XRPD analysis (Figures S6–S10). The crystallographic parameters are summarized in Table 1, and the principal bond distances and angles in the Cd(II) coordination polyhedrons did not differ from the reported values [34]. These are summarized in Table S2, while the H-bonds are given in Table S3. Figures S11–S15 depict the numbering schemes and disordering fragments in **1**–**5.**

Three new compounds with a ddpm chromophore represent a 1D coordination polymer $\{[Cd(OH)(H_2O)(ddpm)_2](BF_4)\}_n$ (**1**), a 2D coordination polymer $\{[Cd(NO_3)(ddpm)_2](H_2O)(NO_3)\}_n$ (**2**), and a supramolecular complex $[Cd(bpy)_2(ddpm)_2](ddpm)(NO_3)_2$ (**3**).

Compound $\{[Cd(OH)(H_2O)(ddpm)_2](BF_4)\}_n$ (**1**) comprises the positively charged polymeric garland chains $\{[Cd(OH)(H_2O)(ddpm)_2]^+\}_n$ (Figure 3a) and the charge-balanced outer-sphere BF_4^- anions. The Cd(II) ion resides on an inversion center in the monoclinic *C*2/*c* space group (Table 1) and has an N_4O_2 with distorted octahedral coordination geometry, originating from four ddpm ligands in the equatorial plane, and one aqua and one hydroxide ligand situated in *trans*-axial positions and statistically alternating in the Cd(II) coordination core with equal probabilities. The ddpm chromophore acts as a bidentate-bridging ligand, thus providing the Cd. . .Cd separation of 12.1589 Å between two consecutive Cd(II) cations within the chain. The ddpm ligand exhibits a standard angular geometry with an interplanar angle between the phenyl rings of 84.1(1)°. This geometry provides a T-shaped arrangement of phenyl rings from two neighboring ddpm ligands within the chains. Similar garland chains were reported for *catena*-(bis(μ_2-ddpm)-diaqua-nickel dichloride) [15] and *catena*-(bis(μ_2-ddpm)-bis(isothiocyanato)-nickel(II)) [16], the closest structural analogs of **1**. The coordination chains in **1** are extended along the crys-

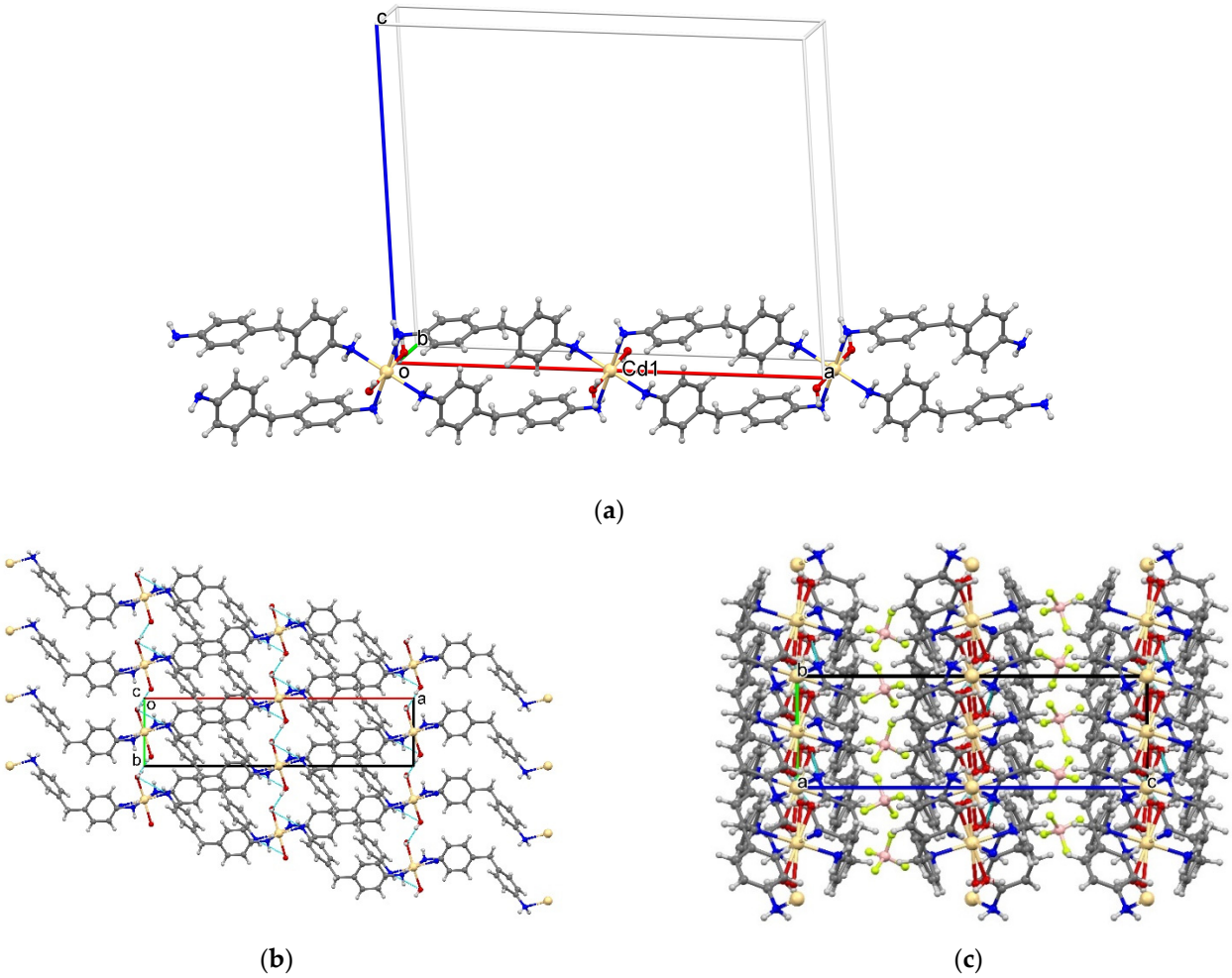
tallographic *a* axis (Table 1), and along the crystallographic *b* axis, they are self-assembled in the H-bonded layer parallel to the (0 0 −1) crystallographic plane via an OH. . .O(H_2O) hydrogen bond (Figure 3b). In the H-bonded layer, the Cd. . .Cd separation via the OH. . .H_2O bridge is 5.9097 Å. The BF_4^- anions are situated between these layers (Figure 3c) and link them in the 3D H-bonded network via NH. . .F hydrogen bonds with participation of amino ligands and CH. . .F short contacts (Table S3).

Table 1. Crystal data and structural refinement parameters for **1**–**5**.

Compound	**1**	**2**	**3**	**4**	**5**
CCDC number	2423294	2423295	2332080	2423296	2423297
Empirical formula	$C_{26}H_{31}BCdF_4N_4O_2$	$C_{26}H_{30}CdN_6O_7$	$C_{59}H_{58}CdN_{12}O_6$	$C_{38}H_{32}CdCl_2N_6O_8$	$C_{44}H_{33.50}CdCl_2N_{7.50}O_8$
FW (g mol^{-1})	630.76	650.96	1143.57	884.01	978.58
Crystal system	monoclinic	orthorhombic	triclinic	triclinic	triclinic
Space group	*C*2/*c*	*Pnma*	*P*-1	*P*-1	*P*-1
a/Å	23.5888(8)	19.5161(5)	12.2860(7)	10.9317(5)	13.0433(9)
b/Å	5.9097(2)	21.6880(7)	13.7458(7)	11.1640(5)	13.0998(9)
c/Å	18.6485(8)	6.3941(2)	19.1891(10)	16.4121(7)	13.5835(9)
α/deg	90	90	105.155(5)	78.883(4)	89.028(5)
β/deg	93.629(3)	90	91.482(4)	77.982(4)	75.710(6)
γ/deg	90	90	115.670(5)	79.885(4)	74.084(6)
V/Å^3	2594.44(17)	2706.40(14)	2783.0(3)	1903.05(14)	2159.7(3)
Z	4	4	2	2	2
D_{calcd} g/cm^3	1.615	1.598	1.365	1.543	1.505
μ/mm^{-1}	0.903	0.864	0.455	0.775	0.692
F(000)	1280	1328	1184	896	992
Reflections collected	4618	6470	18163	12489	13666
Independent reflections	2404 [*R*(int) = 0.0177]	2586 [*R*(int) = 0.0247]	10334 [*R*(int) = 0.0353]	7067 [*R*(int) = 0.0296]	7647 [*R*(int) = 0.0475]
Data/restraints/parameters	2404/79/227	2586/11/230	10334/37/767	7067/103/556	7647/127/628
GOF	1.070	1.141	0.988	1.024	0.952
R_1, wR_2 ($I > 2\sigma(I)$)	0.0347, 0.0864	0.0355, 0.0718	0.0522, 0.0834	0.0435, 0.0936	0.0762, 0.1718
R_1, wR_2 (all data)	0.0467, 0.0960	0.0424, 0.0745	0.0927, 0.0975	0.0615, 0.1032	0.1548, 0.2117
Largest diff. peak and hole	0.549 and −0.474	0.559 and −0.485	0.370 and −0.315	0.387 and −0.384	0.556 and −0.773

Compound {[Cd(NO_3)(ddpm)$_2$](H_2O)(NO_3)}$_n$ (**2**), similarly to **1**, represents an ionic structure. It comprises the positively charged 2D coordination arrays {[Cd(NO_3)(ddpm)$_2$]$^+$}$_n$ and the outer-sphere charge-balanced nitrate anions and water molecules (Figure 4a). Similarly to **1**, the ddpm chromophores act in the bidentate-bridging modes generating garland chains running along the crystallographic *b* axis, thus providing the Cd. . .Cd separation across the ddpm ligands of 12.144 Å. The ddpm linker retains a twisted shape with an interplanar angle between the phenyl rings of 89.1(2)°. The coordination geometry of the Cd(II) ion can be considered as a distorted octahedral, although each Cd(II) cation has an N_4O_3 coordination environment originating from four ddpm ligands situated in the equatoreal plane, as well as nitrate anions in two *trans*-axial positions. The nitrate anion that is disordered by the mirror plane (Table 1) alternatively coordinates in the monodentate and the bidentate-chelate coordination modes; in the latter case, these two oxygen atoms are accepted as occupying one coordination site in the Cd(II) coordination core. Thus, the bridging nitrate anion acts as a tridentate ligand in the monodentate and bidentate-chelate binding modes. The same bridging function of the nitrate group was

registered in *catena*-((μ_2-nitrato-)–bis(4-aminosalicylic acid-silver) [35]. The Cd. . .Cd separation across the nitrate anion in the coordination layer is 6.3941 Å, being longer than through the water–hydroxyl bridge in **1** (see above). The positively charged coordination layers in **2** are interlinked via outer-sphere nitrate anions and water molecules, which are involved in the hydrogen bonds with amino groups (Figure 4b,c, Table S3).



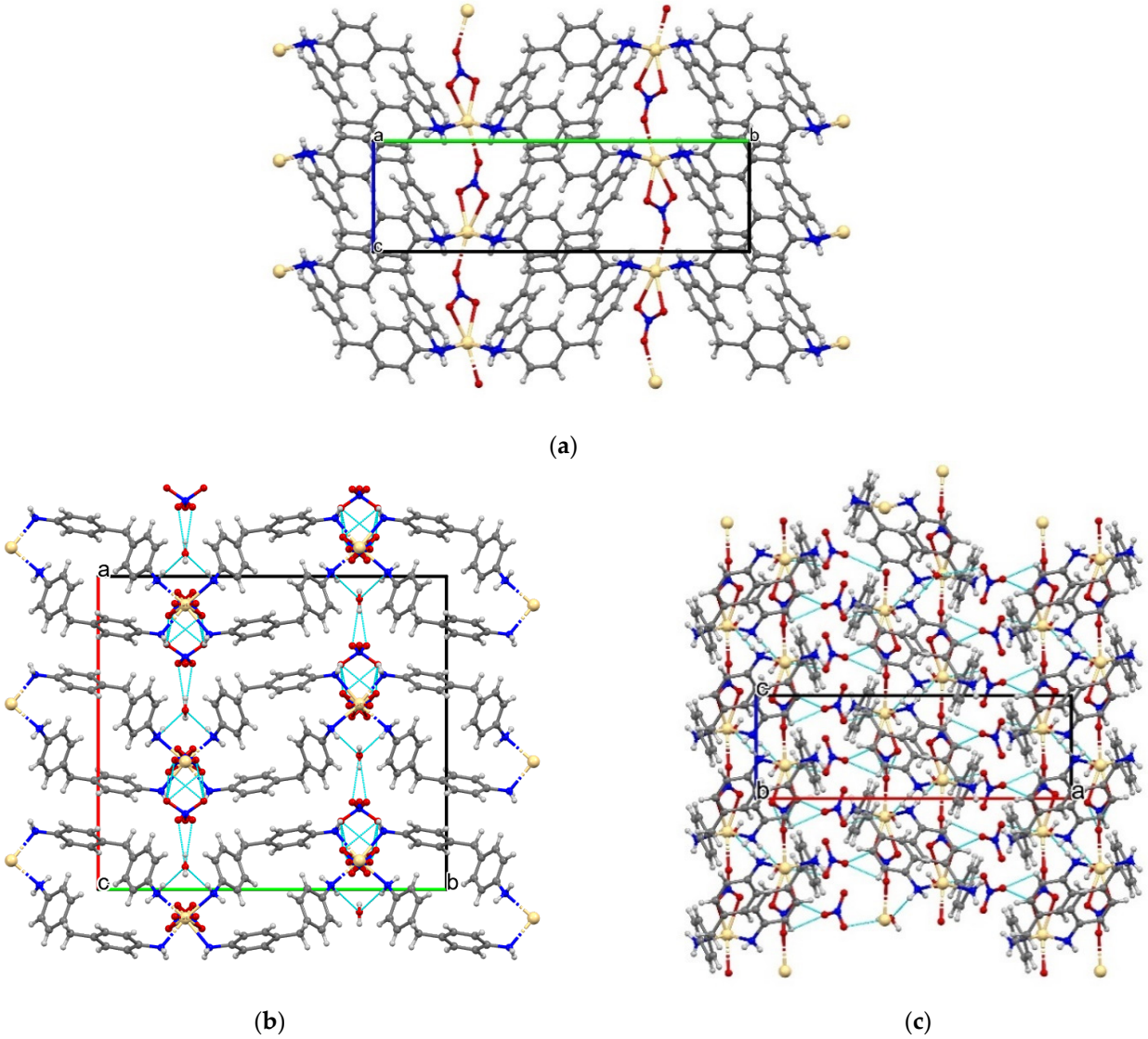
(**a**)

(**b**) (**c**)

Figure 3. Structure of **1**. (**a**) Fragment of 1D coordination chain, (**b**) H-bonded layer generated via OH. . .O hydrogen bonds, and (**c**) crystal packing.

The supramolecular complex $[Cd(bpy)_2(ddpm)_2](NO_3)_2(ddpm)$ **3** comprises a mononuclear $[Cd(bpy)_2(ddpm)_2]^{2+}$ cation, outer-sphere charge-balanced nitrate anions, and ddpm as an inclusion guest molecule (Figure 5a and Figure S13). The Cd(II) cation occupies a general position and has an octahedral N_6-coordination geometry originating from two bidentate-chelate bpy ligands and two monodentate ddpm ligands. The identical ligands are situated in *cis*-positions. The angular fragment $[Cd(bpy)_2]^{2+}$ [27] has a butterfly shape with an interplanar angle between the two chelato-bpy residues of 79.52(6)°. The Cd-coordinated and outer-sphere ddpm molecules are in less strained conformations compared with **1** and **2**, as indicated by the Ph/Ph interplanar angles of 60.4(1), 72.7(1), and 75.2(1)°. The ddpm dangling ligands provide the bulkiness of the complex cation, leading to a linear distance of 20.344(6) Å between the terminal amino groups. The structural study revealed the intramolecular ddpm/bpy π. . .π stacking interactions in the cation, indicated by two shortened distances, Cg(Ph). . .Cg(Py), with 3.782(2) Å, and Cg(Ph). . .Cg (5-membered chelate ring), with 3.467(2) Å. The crystal packing is reinforced by an extensive H-bonded system (Table S3), where two nitrate anions are involved in two interconnect-

ing H-bonded motifs (Figure 5b). One nitrate anion (denoted as N11) is entrapped by four $[Cd(bpy)_2(ddpm)_2]^{2+}$ complex cations and is involved in multiple NH…O hydrogen bonds, acting as a double and triple H-acceptor (Figure S16a) and thus providing the positively charged H-bonded layer $\{[Cd(bpy)_2(ddpm)_2](NO_3)\}^+_n$ (Figure S16b). The second (disordered) nitrate anion and the outer-sphere ddpm molecule are associated in the negatively charged infinite H-bonded motif, $\{(ddpm)(NO_3)\}^-_n$ (Figure S16c); these two motifs alternate and interconnect in the crystal via weaker CH…O contacts (Figure 5b).

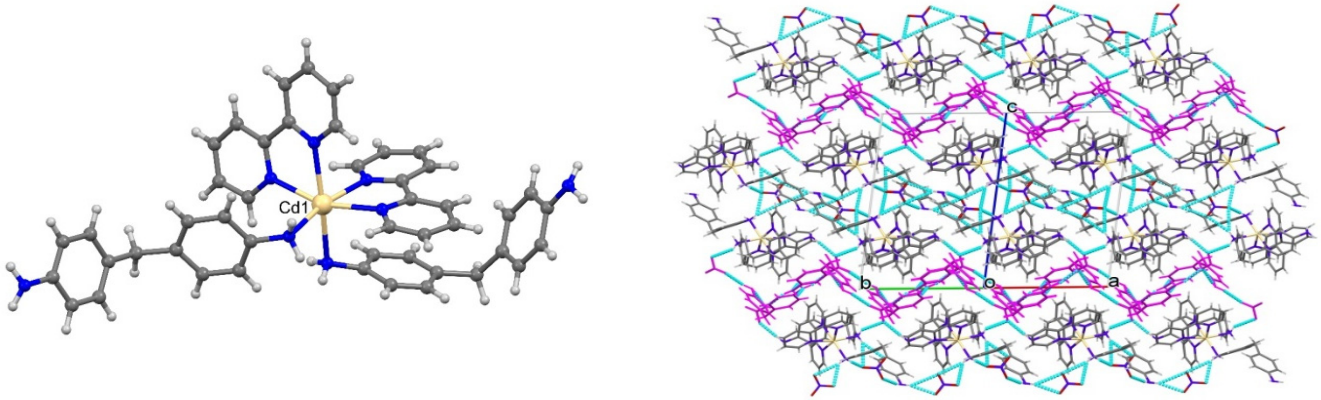


(**a**)

(**b**) (**c**)

Figure 4. Structure of **2**. (**a**) Fragment of 2D coordination grid, (**b**) interconnection of coordination layers via outer-sphere nitrate anions and water molecules, view along the *c*-axis, (**c**) crystal packing, and view along the *b*-axis.

Two new compounds with a ddpe chromophore represent a 1D coordination polymer $\{[Cd(phen)_2(ddpe)](ClO_4)_2\}_n$ (**4**) and a supramolecular complex $[Cd(phen)_3](ClO_4)_2(ddpe)_{0.5}(CH_3CN)_{0.5}$ (**5**).

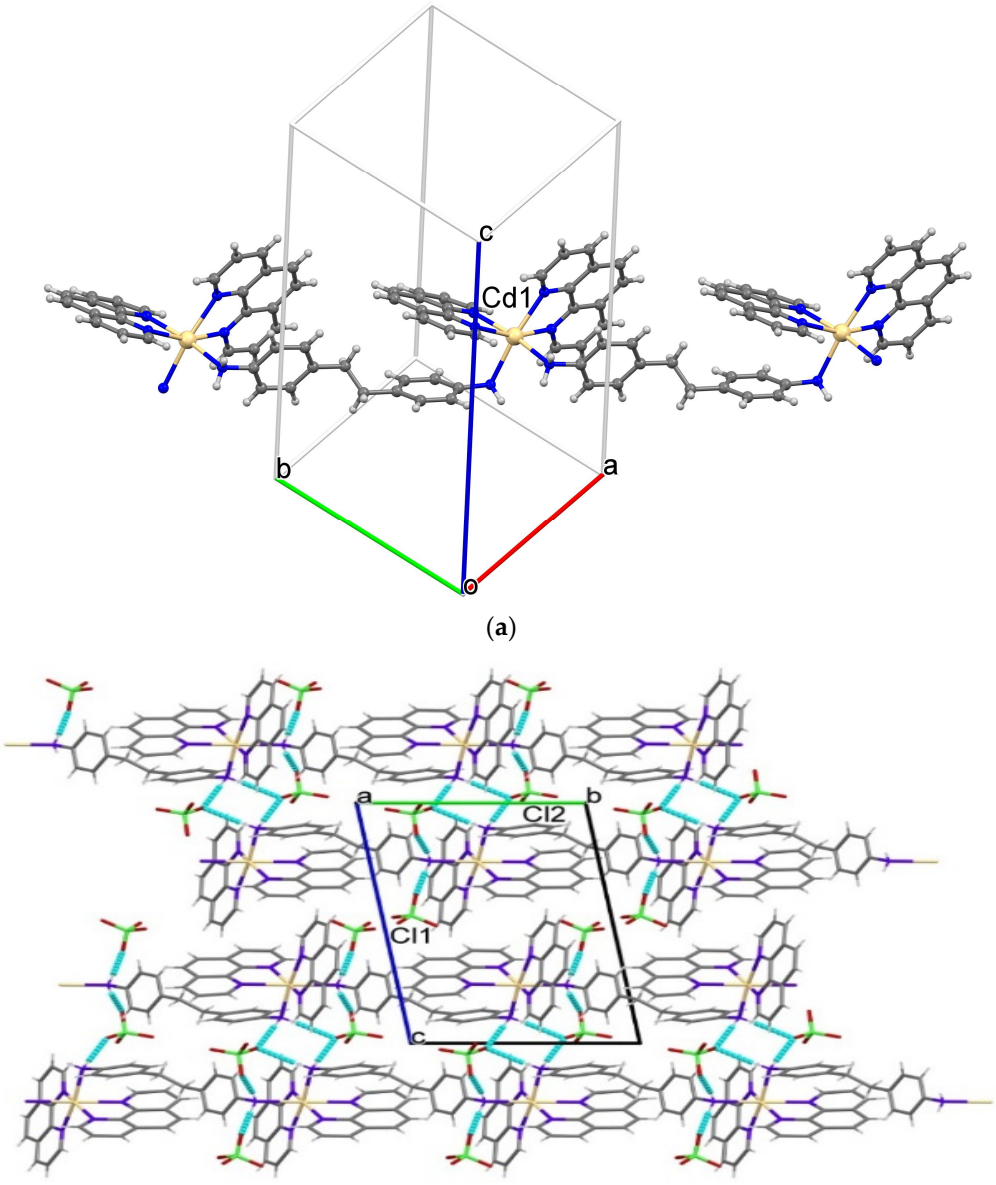


(**a**) (**b**)

Figure 5. Structure of **3**. (**a**) View of mononuclear complex cation $[Cd(bpy)_2(ddpm)_2]^{2+}$ and (**b**) alternation of 2D H-bonded layer motifs. Motif $\{(ddpm)(H_2O)\}_n$ is shown in magenta color.

The 1D coordination polymer **4** comprises linear positively charged coordination chains $\{[Cd(phen)_2(ddpe)]^{2+}\}_n$ (Figure 6a) and outer-sphere charge-balanced perchlorate anions. Each Cd(II) cation has an N_6-octahedral coordination geometry, provided by two bidentate-chelate phen ligands and two bidentate-bridging ddpe ligands. The identical ligands are situated in adjacent positions, and the two terminal phen ligands provide the $[Cd(phen)_2]^{2+}$ corner fragment [28], with an interplanar phen/phen angle of 66.58(6)°. The Cd. . .Cd separation across the ddpe ligand within the chain, which is 14.1870(8) Å. The conformational flexibility of ddpe provides an opportunity for the intrachain heteromeric π. . .π stacking, with the separations Cg(Ph). . .Cg(metallochelate), which is 3.561(2) Å, and Cg(Ph). . .Cg(Py), which is 3.805(2) Å. Each two antiparallel chains are doubled via *a* cyclic H-bonded pattern with participation of two amino groups and two ClO_4^- anions, and the second ClO_4^- anion is also attached to the coordination chain via the NH. . .O hydrogen bond (Figure 6b). Note that compound **4** is only the fourth example of a coordination polymer with the ddpe as a bidentate-bridging ligand, along with the 1D and 2D coordination arrays, *catena*-[(μ_2-ddpe)-(nitrato)-bis(N,N-dimethylformamide)-zinc(II) nitrate], *catena*-[(μ_2-ddpe)-bis(2,2′-bipyridine)-cadmium(II) bis(perchlorate)] and *catena*-[(μ_2-ddpe)-(μ_2-adipato)-cadmium(II) adipic acid], that were recently reported by us [20].

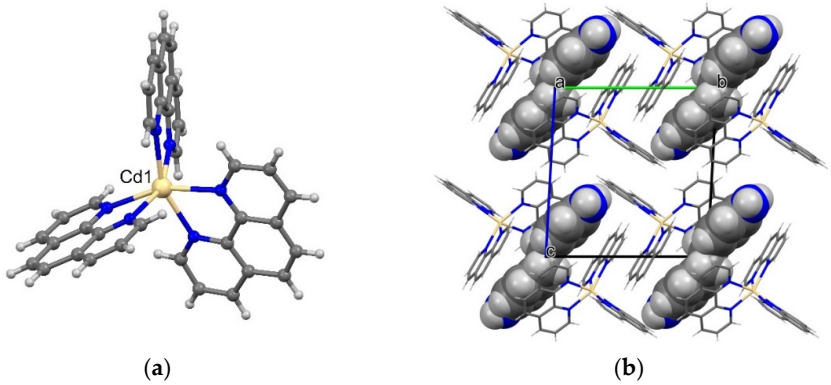
The crystal $[Cd(phen)_3](ClO_4)_2(ddpe)_{0.5}(CH_3CN)_{0.5}$ (**5**) comprises mononuclear cations $[Cd(phen)_3]^{2+}$, outer-sphere perchlorate anions, and ddpe and MeCN neutral molecules. The competition between 1,10-phen and ddpe resulted in the phen ligand coordinating to Cd(II) as a stronger N-base, while the ddpe is accommodated as a guest in the crystal lattice. In the $[Cd(phen)_3]^{2+}$ complex cation, cadmium takes an octahedral N_6-coordination geometry from three bidentate-chelate phen ligands (Figure 7a). The architecture of the three-blade cation $[Cd(phen)_3]^{2+}$ resembles $[Cd(2,2'\text{-bpy})_3]^{2+}$ in the $[Cd(2,2'\text{-bpy})_3](ClO_4)_2]_2(ddpe)(4,4'\text{-bpy})$ analog [20]. The π. . .π stacking interactions were found between the phen wings of the complex cations $[Cd(phen)_3]^{2+}$, Cg(Py1). . .Cg(Py1) 3.448(6) Å, with slippage of 0.423 Å; Cg(chelate ring). . .Cg(Py1) 4.287(5) Å, with slippage 2.646 Å; and Cg(Py2). . .Cg(Py2) 3.752(6), with slippage 1.287 Å, whose alternation results in the 1D stacking columns. The association of these columns forms cavities where the ddpe chromophores reside (Figure 7b), holding in these cavities by numerous π. . .π stacking interactions, with the shortest separations below 5 Å Cg(Ph). . .Cg(phen) being in the range of 4.161(7)–4.939(6) Å, and the N-H. . .π contact being NH. . .C(18) 2.84 Å. Weak NH. . .O and CH. . .O interactions were registered (Table S3), although lipophilic interactions have a significant impact on the crystal packing.



(**a**)

(**b**)

Figure 6. Structure of **4**. (**a**) Fragment of positively charged coordination chain; (**b**) fragment of crystal packing showing the mode of association of adjacent coordination arrays via ClO_4^- anions.



(**a**) (**b**)

Figure 7. Structure of **5**. (**a**) View of $[Cd(phen)_3]^{2+}$ cation and (**b**) mode of inclusion of ddpe chromophore in the crystal lattice. ClO_4^- anions and MeCN molecules were omitted for clarity.

2.4. Photoluminescence Properties

The photoluminescence (PL) properties were studied under ambient conditions for crystals **1**–**5** and compared with the free chromophores ddpm, ddpe, and phen. The close-shell d^{10} Cd(II) metal cation is hard to oxidize, so the ligand-centered (LC) transitions should dominate in all products [29,36] and be redistributed compared to the free ligands under the same conditions due to the versatility of their luminescent levels [22–26,37]. The general trends disclosed in this research corroborate well with our previous findings [19,21]. Two dianiline chromophores revealed very high emission levels in the violet region of the spectrum, with the strong emission maximum at λ_{em} = 352 nm (3.52 eV) for ddpm and λ_{em} = 394 nm (3.14 eV) for ddpe (Figure 8), and a weak signal registered for ddpm in the low-energy (LE) yellow region of the spectrum with a maximum λ_{em} = 577 nm (2.15 eV). The source of the registered dual emission (DE) for the ddpm luminophore may originate from the presence of the electron-rich amino groups and the conformational flexibility of its hydrocarbon skeleton, manifested in the restricted intramolecular twisting in the solid state. As it follows from the crystallographic section, the conformational twist of the ddpm linker varies within approximately 30°, from 60.4° in supramolecular compound **3** to a virtually orthogonal Ph/Ph arrangement in the rigidified coordination arrays **1** and **2**. The same tendency is valid for ddpe, which is in a linear conformation with the Ph rings in parallel or nearly parallel planes in supramolecular complexes but exhibits strained T-shape conformations in coordination polymers [20]. To tune the PL properties of new coordination compounds, the phen and bpy were used as co-ligands. The phen chromophore revealed broad unstructured PL in the region of 362–407 nm (Table S4), whose intensity was comparable with those of ddpm and ddpe in their pure forms (Figure 8). For coordination compounds **1**–**5**, significant redistribution of PL along the spectrum was registered. The general trend was that for **1**–**5**, the PL was at least three orders of magnitude weaker than that observed for the dianiline chromophores (Figures 9 and 10). The coordination polymers **1** and **2**, based on ddmp, revealed very broad unstructured PL in the range of 377-486 nm, with a maximum λ_{em} = 409 nm (3.03 eV) for **1**, and in the range of 354–442 nm, with a maximum λ_{em} = 415 nm (2.99 eV) for **2**, and with a bathochromic shift in PL maxima in both cases. The coordination compounds **4** and **5**, which comprise the phen/bbpe ligand pairs, both revealed DE in the high-energy (HE) region, with λ_{em} = 386 nm (3.21 eV), a shoulder at λ_{em} = 360 nm (3.44 eV) for **4**, and broad emission in the range of 360 nm (3.44 eV)–417 nm (2.97 eV), with an impact from the chelating phen ligand (Figure 10), as well as broad emission with a maximum in the low-energy (LE) region, with λ_{em} = 579 nm (2.14 eV) for **4** and λ_{em} = 600 nm (2.07 eV) for **5**. Generally, compounds **1**–**5** reveal significant PL quenching, which is atypical for rigid coordination arrays but which has been reported for the CdSe quantum dot—organic complexes with a series of aniline ligands [24]. We can also speculate that the PL quenching in our case may have occurred due to partial Cd(II) passivation through the photo-induced hole/electron transfer mechanism [24].

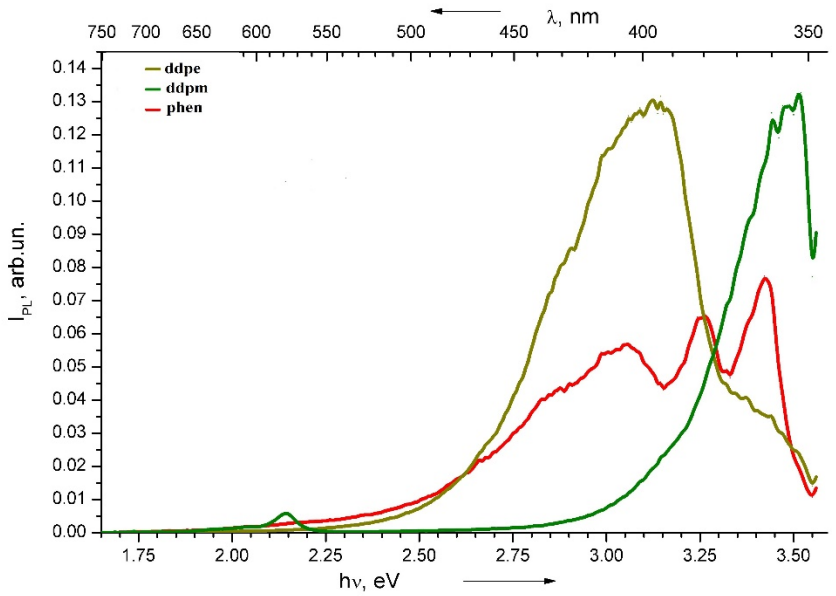


Figure 8. The PL plots for the pure chromophores, ddpe, ddpm, and phen used in this study.

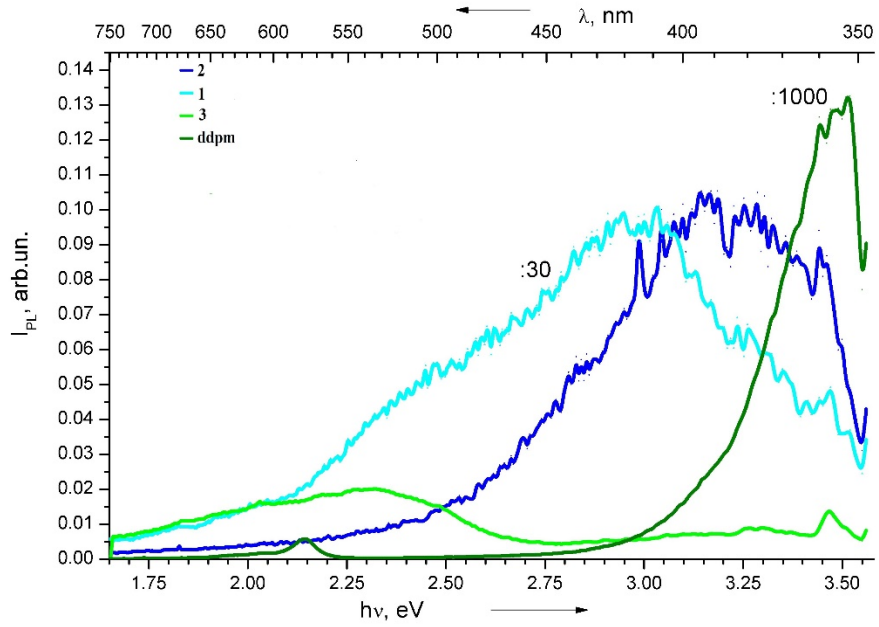


Figure 9. The PL plots for **1**–**3** and ddpm chromophore.

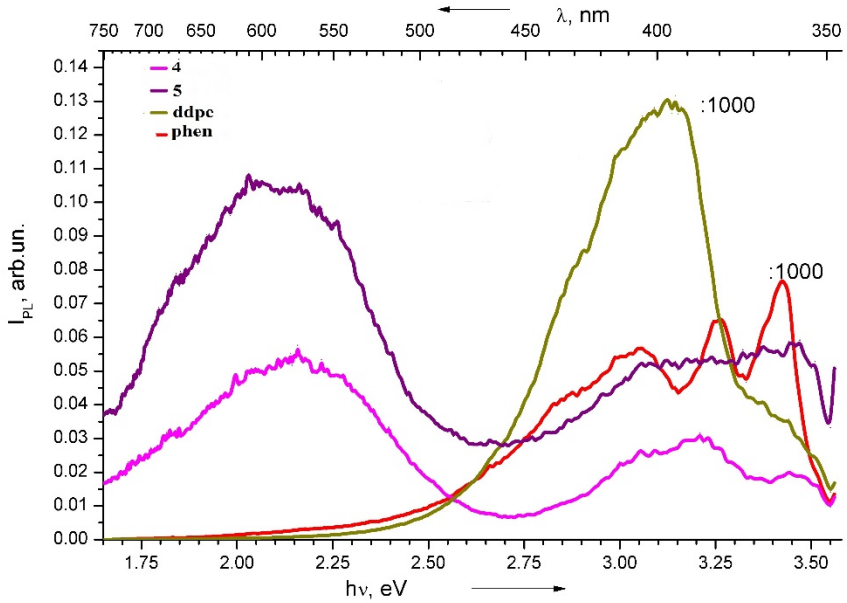


Figure 10. The PL plots for **4** and **5** and ddpe and phen chromophores.

3. Materials and Methods

3.1. Generals

All solvents and chemicals were purchased from commercial sources and used without any purification. The IR(ATR) spectra were recorded on a FTIR Spectrum-100 Perkin Elmer (Perkin Elmer Life & Analytical Sciences, Beaconsfield, UK) spectrometer. Elemental analyses were performed on a Vario EL III Element Analyzer (Elementar Analysensysteme GmbH, Hanau, Germany). The PL was excited by a pulse nitrogen laser (337.1 nm) at room temperature. The excitation pulse duration was 15 ns, the repetition frequency was 50 Hz, and the pulse energy was 0.2 mJ. The radiation was recorded by a photomultiplier tube type FEU-79 (multi-alkaline photocathode, Sb{Na_2K} with an adsorbed cesium layer on the photocathode surface, characteristic S20 type). The recording system's own time was 25 ns. The spectral area was 350–750 nm. The integrity of samples in bulk was checked using X-ray diffraction on a Rigaku MiniFlex 600 (Osaka, Japan) powder diffractometer with CuKα radiation (λ = 1.540598 Å) in a standard 2θ Bragg–Brentano configuration.

3.2. Syntheses

3.2.1. {[$Cd(H_2O)(OH)(ddpm)_2$](BF_4)}$_n$, **1**

A total of 0.04 g (0.2 mmol) of 2,4-diamino-6-phenyl-1,3,5-triazine and 0.03 g (0.15 mmol) of ddpm were dissolved in CH_3CN (5mL) and EtOH (3 mL). Then, 0.029 g (0.1 mmol) of $Cd(BF_4)_2$ $2H_2O$ was added to this solution, and the solution was stirred for 30 min at 80 °C, followed by ultrasonic treatment at 80 °C for 30 min. The brownish crystals precipitated after 180 days. Yield: 0.054 g (86%). Anal. Calcd for $C_{26}H_{31}BCdF_4N_4O_2$: C, 49.52; H, 4.92; N, 8.88%. Found: C, 49.47; H, 4.89; N, 8.86%. IR (cm^{-1}): 33379(m), 2922(s), 1658(w), 1514(s), 1457(m), 1428(s), 1227(m), 1082(s), 1019(m), 986(w), 925(m), 848(s), 722(s), 641(m), 619(s), 532(m).

3.2.2. {[$Cd(NO_3)_2(ddpm)_2$]·(H_2O)}$_n$, **2**

A total of 0.04 g (0.2 mmol) of 2,4-diamino-6-phenyl-1,3,5-triazine and 0.03 g (0.15 mmol) ddpm were dissolved in CH_3CN (4 mL) and MeOH (4 mL). Then, 0.03 g (0.1 mmol) of $Cd(NO_3)_2$·$4H_2O$ was added to this solution. The solution was stirred at 100 °C for 20 min. The yellowish crystals precipitated in 15 days. Yield: 0.045 g (69%). Anal.

Calcd for $C_{26}H_{30}CdN_6O_7$: C, 48; H, 4.61; N, 12.9%. Found: C, 47.95; H, 4.58; N, 12.86%. IR (cm^{-1}): 3443(w), 3332(m), 3276(w), 1652(m), 1595(m), 1511(s), 1475(m), 1438(s), 1318(m), 1281(m), 1193(w), 1079(s), 1015(m), 815(s), 761(s), 735(m), 621(s), 574(s), 512(m), 487(m).

3.2.3. $[Cd(2,2'\text{-bpy})_2(ddpm)_2](ddpm)(NO_3)_2$, **3**

A total of 0.04 g (0.2 mmol) ddpm and 0.02 g (0.1 mmol) 2,2′-bpy were dissolved in EtOH (8 mL). Then, 0.03 g (0.1 mmol) of $Cd(NO_3)_2 \cdot 4H_2O$ was added to this solution. The resulting mixture was heated in a solvothermal reactor at 80 °C for 17 h. The brownish crystals precipitated in 24 h. Yield: 0.054 g (47%). Anal. Calcd for $C_{59}H_{58}CdN_{12}O_6$: C, 61.99; H, 5.07; N, 14.71%. Found: C, 61.95; H, 5.04; N, 14.68%. IR (cm^{-1}): 3329(w), 3156(w), 1580(m), 1514(s), 1428(s), 1343(m), 1226(m), 1146(w), 1090(s), 1054(w), 1019(w), 926(m), 848(s), 825(w), 722(s), 619(s), 532(m).

3.2.4. $\{[Cd(phen)_2(ddpe)](ClO_4)_2\}_n$, **4**

A total of 0.04 g (0.2 mmol) ddpe and 0.02 g (0.1 mmol) phen were dissolved in CH_3CN (4 mL) and EtOH (4 mL). Then, 0.03 g (0.1 mmol) of $Cd(ClO_4)_2$ $2H_2O$ was added to this solution. The resulting mixture was heated in a solvothermal reactor at 80 °C for 17 h. The colorless crystals precipitated in 90 days. Yield: 0.0585 g (66%). Anal. Calcd for $C_{38}H_{32}CdCl_2N_6O_8$: C, 51.64; H, 3.62; N, 9.51%. Found: C, 51.61; H, 3.59; N, 9.48%. IR (cm^{-1}): 3339(w), 3297(w), 1580(m), 1514(s), 1428(s), 1343(m), 1226(m), 1146(w), 1090(s), 1054(w), 1019(w), 926(m), 848(s), 825(w), 722(s), 619(s), 532(m).

3.2.5. $[Cd(phen)_3](ClO_4)(ddpe)_{0.5}(CH_3CN)_{0.5}$, **5**

A total of 0.02 g (0.1 mmol) ddpe and 0.04 g (0.2 mmol) phen were dissolved in CH_3CN (4 mL) and EtOH (4 mL). Then, 0.03 g (0.1 mmol) of $Cd(ClO_4)_2$ $2H_2O$ was added to this solution. The resulting mixture was heated in a solvothermal reactor at 90 °C for 17 h. The colorless crystals precipitated in 90 days. Yield: 0.0495 g (51%). Anal. Calcd. for $C_{44}H_{33.5}CdCl_2N_{7.5}O_8$: C, 53.98; H, 3.42; N, 11.04%. Found: C, 53.95; H, 3.39; N, 11%. IR (cm^{-1}): 3340(w), 1664(s), 1622(w), 1540(w), 1515(s), 1425(s), 1341(m), 1267(w), 1146(m), 1077(s), 845(s), 771(m), 722(s), 621(s).

3.3. Single-Crystal X-Ray Diffraction Studies

The crystal data for **1**–**5** were collected at room temperature on an Xcalibur E diffractometer with a CCD area detector (graphite monochromator, MoKα radiation). The structures were solved and refined using SHELXS and SHELXL [38,39]. The C-bound H-atoms were refined in riding modes with $U_{iso}(H) = 1.2U_{eq}(C)$. The N(O)-bound H-atoms in amino groups and water molecules were located in different Fourier maps and refined using the DFIX instruction (N(O)–H = 0.86 Å) and $U_{iso}(H) = 1.5U_{eq}(O,N)$. The disordered inorganic anions were refined using the idealized tetrahedral geometries for the BF_4^- and ClO_4^- anions and planar trigonal geometry for the NO_3^- anion, as well as the equalized thermal displacement parameters for the similar atoms. The figures were produced using MERCURY [40].

4. Conclusions

In conclusion, the structural diversity of coordination arrays with the participation of two dianiline chromophores has been demonstrated in this study on five new coordination compounds. The availability of two terminal amino groups in the ddpm and ddpe molecules allowed for the assembly of three new coordination polymers, **1**, **2**, and **4**, with 1D and 2D structural motifs, in which both dianiline chromophores manifested their coordination and H-donor properties. The choice of anion was also important, since the well-coordinated tridentate nitrate anion provided an access to a unique 2D coordi-

nation array in **2** and demonstrated powerful H-acceptor properties as double and triple H-acceptors organizing around four bulky Cd(II) complex cations in the case of supramolecular aggregate **3**. The easily leaving BF_4^- and ClO_4^- anions expectedly provided access to the positively charged coordination networks and were also successfully involved in NH. . .F(O) hydrogen bonding networks in **1**, **4**, and **5**. The impact of lipophilic stacking interactions appeared meaningful in the crystals of compounds **3**, **4**, **5** when the bpy and phen ligands coordinated to the metal. The recorded fading of PL in the coordination polymers in comparison with the pure forms of ddpm and ddpe can serve for detection of these chromophores and harmful metals (Cd, etc.) and inorganic anions (NO_3^-, ClO_4^-) in environmental media.

Supplementary Materials: The following supporting information can be downloaded at: https://www.mdpi.com/article/10.3390/inorganics13030090/s1, Table S1: Principal IR bands in **1**–**5** and started chromophores; Table S2: Bond lengths and angles of **1**–**5**; Table S3: Hydrogen bonds in **1**–**5**; Table S4: Positions of emission maxima (λ, E) in the PL spectra of chromophores ddpm, ddpe, phen and compounds **1**–**5**. Figures S1–S5: IR spectra for **1**–**5** and starting ligands; Figures S6–S10: XRPD patterns for **1**–**5**; Figures S11–S15: ORTEP drawings for **1**–**5** with atom numbering schemes and indications of disordering: Figure S16: fragments of crystal packing in **3**. CCDC contains the supplementary crystallographic data for **1**–**5** by quoting the CCDC deposition numbers 2332080 and 2423294–2423297. These data can be obtained free of charge via https://www.ccdc.cam.ac.uk/structures/? or from the Cambridge Crystallographic Data Centre, 12 Union Road, Cambridge CB2 1EZ, UK; fax: (+44) 1223-336-033; or e-mail: deposit@ccdc.cam.ac.uk.

Author Contributions: N.C.: Investigation, Data curation, Visualization, and Original draft writing. E.M.: Investigation, Data curation, Visualization, and Original draft writing. A.V.S.: Investigation, Data curation, and Visualization. N.V.C.: Investigation and Data curation, D.C.: Investigation and Data curation. M.S.F.: Conceptualization, Supervision, and Writing—review and editing. All authors have read and agreed to the published version of the manuscript.

Funding: Subprogram 011202, financed by the Ministry of Education and Research of R. Moldova.

Institutional Review Board Statement: Not applicable.

Informed Consent Statement: Not applicable.

Data Availability Statement: The original contributions presented in the study are included in the article/Supplementary Material, further inquiries can be directed to the corresponding author.

Conflicts of Interest: The authors declare no conflicts of interest.

References

1. Burrows, A.D.; Chan, C.-W.; Chowdhry, M.M.; McGrady, J.E.; Mingos, D.M.P. Multidimensional Crystal Engineering of Bifunctional Metal Complexes Containing Complementary Triple Hydrogen Bonds. *Chem. Soc. Rev.* **1995**, *24*, 329–339. [CrossRef]
2. MacDonald, J.C.; Dorrestein, P.C.; Pilley, M.M.; Foote, M.M.; Lundburg, J.L.; Henning, R.W.; Schultz, A.J.; Manson, J.L. Design of Layered Crystalline Materials Using Coordination Chemistry and Hydrogen Bonds. *J. Am. Chem. Soc.* **2000**, *122*, 11692–11702. [CrossRef]
3. Beatty, A.M. Open-framework coordination complexes from hydrogen-bonded networks: Toward host/guest complexes. *Coord. Chem. Rev.* **2003**, *246*, 131–143. [CrossRef]
4. Pickering, A.L.; Long, D.L.; Cronin, L. Coordination Networks through the Dimensions: From Discrete Clusters to 1D, 2D, and 3D Silver(I) Coordination Polymers with Rigid Aliphatic Amino Ligands. *Inorg. Chem.* **2004**, *43*, 4953–4961. [CrossRef]
5. Đaković, M.; Borovina, M.; Pisačić, M.; Aakeröy, C.B.; Soldin, Ž.; Kukovec, B.-M.; Kodrin, I. Mechanically Responsive Crystalline Coordination Polymers with Controllable Elasticity. *Angew. Chem. Int. Ed.* **2018**, *57*, 14801–14805. [CrossRef] [PubMed]
6. Bhattacharya, B.; Michalchuk, A.A.L.; Silbernagl, D.; Rautenberg, M.; Schmid, T.; Feiler, T.; Reimann, K.; Ghalgaoui, A.; Sturm, H.; Paulus, B.; et al. A Mechanistic Perspective on Plastically Flexible Coordination Polymers. *Angew. Chem. Int. Ed.* **2020**, *59*, 5557–5561. [CrossRef]

7. Yin, M.-R.; Yan, Q.-Q.; Li, B.; Yong, G.-P. 1D ladder and 2D bilayer coordination polymers constructed from a new T-shaped ligand: Luminescence, magnetic and CO_2 gas adsorption properties. *Cryst. Eng. Comm.* **2021**, *23*, 3196–3203. [CrossRef]
8. Sun, N.; Yu, H.; Yu, X.; Jiang, Q.; Wang, Z.; Ding, F.; Potapov, A.S.; Sun, Y. Zinc-based 1D coordination polymer for selective luminescent detection of nitrofuran antibiotics at part-*per*-billion level. *Polyhedron* **2024**, *259*, 117065. [CrossRef]
9. Dong, X.; Li, Y.; Li, D.; Liao, D.; Qin, T.; Prakash, O.; Kumar, A.; Liu, J. A new 3D 8-connected Cd(II) MOF as a potent photocatalyst for oxytetracycline antibiotic degradation. *Cryst. Eng. Comm.* **2022**, *24*, 6933–6943. [CrossRef]
10. Liu, C.-Y.; Chen, X.-R.; Chen, H.-X.; Niu, Z.; Hirao, H.; Braunstein, P.; Lang, J.-P. Ultrafast Luminescent Light-Up Guest Detection Based on the Lock of the Host Molecular Vibration. *J. Am. Chem. Soc.* **2020**, *142*, 6690–6697. [CrossRef]
11. Chisca, D.; Croitor, L.; Coropceanu, E.B.; Petuhov, O.; Volodina, G.F.; Baca, S.G.; Krämer, K.; Hauser, J.; Decurtins, S.; Liu, S.-X.; et al. Six Flexible and Rigid Co(II) Coordination Networks with Dicarboxylate and Nicotinamide-Like Ligands: Impact of Noncovalent Interactions in Retention of Dimethylformamide Solvent. *Cryst. Growth Des.* **2016**, *16*, 7011–7024. [CrossRef]
12. Shao, C.; Chang, H.; Wang, M.; Xu, F.; Yang, J. High-Strength, Tough, and Self-Healing Nanocomposite Physical Hydrogels Based on the Synergistic Effects of Dynamic Hydrogen Bond and Dual Coordination Bonds. *ACS Appl. Mater. Interfaces* **2017**, *9*, 28305–28318. [CrossRef]
13. Wu, X.; Wang, J.; Huang, J.; Yang, S. Robust, Stretchable, and Self-Healable Supramolecular Elastomers Synergistically Cross-Linked by Hydrogen Bonds and Coordination Bonds. *ACS Appl. Mater. Interfaces* **2019**, *11*, 7387–7396. [CrossRef]
14. Li, B.; Cao, P.-F.; Saito, T.; Sokolov, A.P. Intrinsically Self-Healing Polymers: From Mechanistic Insight to Current Challenges. *Chem. Rev.* **2023**, *123*, 701–735. [CrossRef]
15. Carlucci, L.; Ciani, G.; Proserpio, D.H.; Porta, F. New metal–organic frameworks and supramolecular arrays assembled with the bent ditopic ligand 4,4-diaminodiphenylmethane. *Cryst. Eng. Comm.* **2006**, *8*, 696–706. [CrossRef]
16. Yu, W.-J.; Li, X.-M.; Zhang, S.-S. Synthesis and characterization of polymeric Ni(II) complexes of 4-(4-aminobenzyl)benzenamine (abba) and 4-(4-aminophenylthio)benzenamine (aptba) with thiocyanate. *J. Coord. Chem.* **2007**, *60*, 2361. [CrossRef]
17. Luo, J.; Hong, M.; Wang, R.; Cao, R.; Shi, Q.; Weng, J. Self-Assembly of Five Cadmium(II) Coordination Polymers from 4,4′-Diaminodiphenylmethane. *Eur. J. Inorg. Chem.* **2003**, *9*, 1778–1784. [CrossRef]
18. Liu, L.; Huang, S.-P.; Yang, G.-D.; Zhang, H.; Wang, X.-L.; Fu, Z.-Y.; Dai, J.-C. Zn[Htma][ddm]: An Interesting Three-Dimensional Chiral Nonlinear Optical-Active Zinc-Trimesate Framework. *Cryst. Growth Des.* **2010**, *10*, 930–936. [CrossRef]
19. Chisca, D.; Croitor, L.; Melnic, E.; Petuhov, O.; Kulikova, O.; Fonari, M.S. Six transition metal–organic materials with the ditopic 4,4′-diaminodiphenylmethane ligand: Synthesis, structure characterization and luminescent properties. *Polyhedron* **2020**, *192*, 114844. [CrossRef]
20. Craciun, N.; Chisca, D.; Melnic, E.; Fonari, M.S. Unprecedented Coordination Compounds with 4,4′-Diaminodiphenylethane as a Supramolecular Agent and Ditopic Ligand: Synthesis, Crystal Structures and Hirshfeld Surface Analysis. *Crystals* **2023**, *13*, 289. [CrossRef]
21. Craciun, N.; Melnic, E.; Kulikova, O.V.; Siminel, A.V.; Chisca, D.; Fonari, M.S. Interplay of bipyridine and 4,4′-diaminodiphenylmethane ligands in crystal design of cadmium-based coordination polymers: Structures and unusual photoluminescence quenching. *Polyhedron* **2024**, *251*, 116850. [CrossRef]
22. Zhang, S.; Huang, M.; Lu, H.; Ma, Z.; Wang, Z.; Yang, J. Three-arm star-shaped aniline derivatives: Tunable photoluminescence, aggregation-induced emission and reversible acid-base vapor fluorescence response. *J. Photochem. Photobiol. A Chem.* **2022**, *432*, 114098. [CrossRef]
23. Jhang, W.R.; Lai, H.Y.; Lin, Y.-C.; Lee, C.; Lee, S.-H.; Lee, Y.-Y.; Chi-Kung Ni, C.-K.; Tsen, C.-M. Triplet vs $\pi\sigma*$ state mediated N–H dissociation of aniline. *J. Chem. Phys.* **2019**, *151*, 141101. [CrossRef]
24. Knowles, K.E.; Tice, D.B.; McArthur, E.A.; Solomon, G.C.; Weiss, E.A. Chemical Control of the Photoluminescence of CdSe Quantum Dot-Organic Complexes with a Series of Para-Substituted Aniline Ligands. *J. Am. Chem. Soc.* **2010**, *132*, 1041–1050. [CrossRef] [PubMed]
25. Kwon, W.; Do, S.; Kim, J.H.; Jeong, M.S.; Rhee, S.-W. Control of Photoluminescence of Carbon Nanodots via Surface Functionalization using Para-substituted Anilines. *Sci. Rep.* **2015**, *5*, 12604. [CrossRef]
26. Ghosh, T.; Chatterjee, S.; Prasad, E. Photoinduced Electron Transfer from Various Aniline Derivatives to Graphene Quantum Dots. *J. Phys. Chem. A* **2015**, *119*, 11783–11790. [CrossRef] [PubMed]
27. Melnic, E.; Coropceanu, E.B.; Forni, A.; Cariati, E.; Kulikova, O.V.; Siminel, A.V.; Kravtsov, V.C.; Fonari, M. Discrete Complexes and One-Dimensional Coordination Polymers with $[Cu(II)(2,2'\text{-bpy})]^{2+}$ and $[Cu(II)(phen)]^{2+}$ Corner Fragments: Insight into Supramolecular Structure and Optical Properties. *Cryst. Growth Des.* **2016**, *16*, 6275–6285. [CrossRef]
28. Melnic, E.; Coropceanu, E.B.; Kulikova, O.V.; Siminel, A.V.; Anderson, D.; Rivera-Jacquez, H.J.; Masunov, A.E.; Fonari, M.S.; Kravtsov, V.C. Robust Packing Patterns and Luminescence Quenching in Mononuclear $[Cu(II)(phen)_2]$ Sulfates. *J. Phys. Chem. C* **2014**, *118*, 30087–30100. [CrossRef]
29. Accorsi, G.; Listorti, A.; Yoosaf, K.; Armaroli, N. 1,10-Phenanthrolines: Versatile building blocks for luminescent molecules, materials and metal complexes. *Chem. Soc. Rev.* **2009**, *38*, 1690–1700. [CrossRef]

30. David, A.; Thornton, D.A. Metal Complexes of Aniline: Infrared and Raman Spectra. *J. Coord. Chem.* **1991**, *24*, 261–289. [CrossRef]
31. Yamada, T.; Mizuno, M. Infrared and Terahertz Spectroscopic Investigation of Imidazolium, Pyridinium, and Tetraalkylammonium Tetrafluoroborate Ionic Liquids. *ACS Omega* **2022**, *7*, 29804–29812. [CrossRef] [PubMed]
32. Gatehouse, B.M.; Livingstone, S.E.; Nyholm, R.S. 847. Infrared spectra of some nitrato-co-ordination complexes. *J. Chem. Soc.* **1957**, 4222–4225. [CrossRef]
33. Fogaça, L.A.; Bereczki, L.; Petruševski, V.M.; Barta-Holló, B.; Franguelli, F.P.; Mohai, M.; Béres, K.A.; Sajó, I.E.; Szilágyi, I.M.; Kotai, L. A Quasi-Intramolecular Solid-Phase Redox Reaction of Ammonia Ligands and Perchlorate Anion in Diamminesilver(I) Perchlorate. *Inorganics* **2021**, *9*, 38. [CrossRef]
34. Groom, C.R.; Bruno, I.J.; Lightfoot, M.P.; Ward, S.C. The Cambridge Structural Database. *Acta Cryst. B* **2016**, *72*, 171–179. [CrossRef] [PubMed]
35. Braga, D.; Grepioni, F.; Andre, V.; Duarte, M.T. Drug-containing coordination and hydrogen bonding networks obtained mechanochemically. *Cryst. Eng. Comm.* **2009**, *11*, 2618–2621. [CrossRef]
36. Barbieri, A.; Accorsi, G.; Armaroli, N. Luminescent complexes beyond the platinum group: The d10 avenue. *Chem. Commun.* **2008**, 2185–2193. [CrossRef]
37. Pal, T.K.; Mallik, G.K.; Laha, S.; Chatterjee, K.; Ganguly, T.; Banerjee, S.B. Electronic emission and absorption spectra and the effect of hydrogen bonding on the ground and excited electronic states of some anilines. *Spectrochim. Acta. Part. A Mol. Spectroscopy* **1987**, *43A*, 853–859. [CrossRef]
38. Sheldrick, G.M. A short history of SHELX. *Acta Cryst.* **2008**, *A64*, 112–122. [CrossRef]
39. Sheldrick, G.M. Crystal structure refinement with SHELXL. *Acta Cryst.* **2015**, *C71*, 3–8. [CrossRef]
40. Macrae, C.F.; Bruno, I.J.; Chisholm, J.A.; Edgington, P.R.; McCabe, P.; Pidcock, E.; Rodriguez-Monge, L.; Taylor, R.; Streek, J.; Wood, P.A. Mercury CSD 2.0—New features for the visualization and investigation of crystal structures. *J. Appl. Cryst.* **2008**, *41*, 466–470. [CrossRef]

Disclaimer/Publisher's Note: The statements, opinions and data contained in all publications are solely those of the individual author(s) and contributor(s) and not of MDPI and/or the editor(s). MDPI and/or the editor(s) disclaim responsibility for any injury to people or property resulting from any ideas, methods, instructions or products referred to in the content.